The stability of an evolving Atlantic meridional overturning circulation

Wei Liu,[1,2] Zhengyu Liu,[3,2] and Aixue Hu[4]

Received 30 January 2013; revised 13 March 2013; accepted 14 March 2013; published 23 April 2013.

[1] In this study, we propose a generalized stability indicator, L, for a slowly evolving and quasi-steady Atlantic meridional overturning circulation (AMOC), which represents a feedback related to the AMOC and its associated freshwater transport within the Atlantic basin. As an improvement from previous indicators for the AMOC in equilibrium, this generalized indicator does not require a divergence-free freshwater transport in the Atlantic for a collapsed AMOC, which enables it to correctly monitor the AMOC stability through the AMOC hysteresis loop in the coupled atmosphere-ocean general circulation models. From the simulation, the indicator L suggests that the AMOC is in a stable regime, with single equilibrium under the present-day and the Last Glacial Maximum (LGM) climates. However, under the present-day climate, a Bering Strait (BS) closure will diminish the freshwater outflow from the North Atlantic into the Arctic as the AMOC collapses, resulting in a freshwater convergence in the Atlantic basin and making the AMOC reside in a stable collapsed state, i.e., the AMOC exhibits characteristics of multiple equilibria. Further analysis shows that the BS effect is much reduced under the LGM climate. This generalized indicator L has great implications for paleoclimate studies in understanding the abrupt climate change due to the instability of the AMOC.
Citation: Liu, W., Z. Liu, and A. Hu (2013), The stability of an evolving Atlantic meridional overturning circulation, *Geophys. Res. Lett., 40*, 1562–1568, doi:10.1002/grl.50365.

1. Introduction

[2] The Atlantic meridional overturning circulation (AMOC) plays an important role in the Northern Hemisphere climate [*Ganachaud and Wunsch*, 2000]. However, as a highly nonlinear system, it is very sensitive to the freshwater forcing and may exhibit sudden changes as induced by the instability in the circulation system. Paleoclimate evidence shows that abrupt climate transitions, such as Dansgaard-Oeschger cycles [*Dansgaard et al*., 1993], are closely related to the sudden changes in the AMOC due to the input of the freshwater discharged from the ice sheet melting [*Broecker et al*., 1985; *Bond et al*., 1997]. Therefore, a better understanding of the AMOC stability properties will shed light on our comprehension about the status of past, present, and future climates.

[3] The stability properties of the AMOC have been extensively investigated in simple box models [e.g., *Stommel*, 1961; *Rooth*, 1982; *Tziperman et al*., 1994], ocean general circulation models [e.g., *Bryan*, 1986; *Marotzke et al*., 1988; *Weaver and Sarachik*, 1991], Earth system models of intermediate complexity [e.g., *Rahmstorf et al*., 2005; *Hofmann and Rahmstorf*, 2009], and some coupled atmosphere-ocean general circulation models (CGCMs) [e.g., *Manabe and Stouffer*, 1988; *Yin and Stouffer*, 2007; *Hawkins et al*., 2011]. According to these studies, the AMOC is found to have two equilibrium states: the "conveyor belt" and "collapsed" states. When a threshold is exceeded, an irreversible transition may occur between two states so that the circulation will exhibit significant hysteresis behaviors [e.g., *Rahmstorf*, 1995; *Rahmstorf et al*., 2005; *Hawkins et al*., 2011; *Hu et al*., 2012a].

[4] Meanwhile, diagnostic indicators have been developed to monitor the stability of the AMOC. *Rahmstorf* [1996] first proposed a transport indicator, M_{ovS}, the freshwater transport by the overturning circulation across the southern boundary of the Atlantic, as a diagnostic indicator of the AMOC stability. Further studies showed that this transport indicator should be refined to be a convergence indicator ΔM_{ov} that consists of the net freshwater transport by the AMOC within the Atlantic between the southern and northern boundaries [*Dijkstra*, 2007; *Huisman et al*., 2010; *Liu and Liu*, 2013; *Liu*, 2012]. These indicators, however, are based on an active AMOC in equilibrium and are not valid for an evolving circulation [*Hawkins et al*., 2011]. On the other hand, paleoclimate records suggest that the real AMOC has never kept a perfect equilibrium in the past climate [e.g., *Severinghaus and Brook*, 1999; *McManus et al*., 2004]. During most periods, it appears as a slowly evolving circulation in a quasi-equilibrium state. Therefore, a stability indicator is highly needed for the slowly evolving and quasi-steady AMOC, especially in the context of paleoclimatology.

[5] In this paper, we report a generalized stability indicator for a slowly evolving AMOC. By using it, for the first time, we correctly monitor the AMOC stability through the AMOC hysteresis loops in CGCMs. Besides, for the AMOC in equilibrium, this generalized stability indicator can correctly indicate the AMOC stability as the AMOC transits from one equilibrium to another.

All supporting information may be found in the online version of this article.

[1]Key Laboratory of Meteorological Disaster of Ministry of Education, School of Marine Sciences, Nanjing University of Information Science & Technology, Nanjing, China.
[2]Center for Climatic Research, University of Wisconsin-Madison, Madison, Wisconsin, USA.
[3]Laboratory Climate, Ocean and Atmosphere Studies, Peking University, Beijing, China.
[4]Climate and Global Dynamics Division, National Center for Atmospheric Research, Boulder, Colorado, USA.

Corresponding author: W. Liu, Key Laboratory of Meteorological Disaster of Ministry of Education, School of Marine Sciences, Nanjing University of Information Science & Technology, Nanjing, China. (wliu5@wisc.edu)

0094-8276/13/10.1002/grl.50365

2. Model and Experiments

[6] The state-of-the-art CGCMs used in this study are two versions of the National Center for Atmospheric Research (NCAR) Community Climate System Model version 3 (CCSM3): a standard T42 version, i.e., CCSM3 T42 [*Collins et al*., 2006], and a low-resolution T31 version, i.e., CCSM3 T31 [*Yeager et al*., 2006] (SI text 1). Two AMOC hysteresis experiments are based on CCSM3 T42 under the present-day boundary conditions, in which everything is identical except one with an open Bering Strait (OBS) and the other with a closed Bering Strait (CBS) [*Hu et al*., 2012a,2012b]. Following *Rahmstorf et al*. [2005], additional freshwater forcing of 200 m^3/s is uniformly distributed in the North Atlantic within 20–50°N, and it increases by 200 m^3 s per year until the AMOC collapses, i.e., year 2200 in OBS and year 2100 in CBS. After that, the additional freshwater forcing linearly decreases to zero at the same rate. With such a slow rate change, it will take 500 years for the freshwater forcing to reach an increment/decrement of 0.1 Sv. As a result, the AMOC can be kept in a quasi-equilibrium state throughout the whole simulation.

[7] The third AMOC hysteresis experiment (LGM) is performed in CCSM3 T31 under the Last Glacial Maximum (LGM) condition. It starts from a LGM state of 19.0 ka B.P. in a transient simulation of last deglaciation [*Liu et al*., 2009] and keeps constant orbital forcing and greenhouse gas concentration at 19.0 ka B.P. in the experiment. Slightly different from OBS and CBS, the freshwater discharge in LGM is uniformly distributed in the North Atlantic within 50–70°N, which starts from zero and increases by 86 m^3 s per year until the AMOC collapses at year 2000. Then, this freshwater discharge reduces linearly by 86 m^3/s per year. Despite a different hosing scheme, the hosing rate in LGM is very close to that of OBS and CBS in the same region since, in the latter two cases, about half of the freshwater input within 20–50°N is swept northward by the meridional Ekman transport, resulting in a hosing rate within 50–70°N of about 100 m^3 s per year.

[8] Here it is worth interpreting the difference in the hosing region among three cases. In OBS and CBS, the hosing region is selected as 20–50°N in the Atlantic to examine the "advective instability" of the AMOC, without directly applying the freshwater over the deepwater formation areas. The LGM simulation, however, is in the context of a transient simulation of the last deglaciation [*Liu et al*., 2009]. So, in this experiment, meltwater flux is input within the latitude band 50–70°N across the Atlantic for simulating the freshwater discharge due to the ice sheet retreat. One issue for this hosing region is that it is over the deepwater formation area so that a second instability, the "convective instability," may be induced. As a result, in the case of a bistable AMOC with a robust hysteresis behavior, the circulation will switch off altogether in a sudden step due to the "convective instability," as opposed to the more gradual "advective shutdown." While for a monostable AMOC, such as the LGM case in this study, the "convective instability" has little effect. In brief, although the hosing region is a bit different among three experiments, the anomalous freshwater flux can always be advected through the path of the AMOC for testing the basin-scale advective salinity feedback [*Stommel*, 1961].

3. Results

[9] Figure 1 shows the AMOC hysteresis diagrams among three experiments, in which the AMOC strength ψ is defined as the maximum of the annual overturning streamfunction below 500 m depth within the North Atlantic. In the OBS and LGM simulations, the AMOC hysteresis loops are not significant. In each case, the AMOC winds down with increasing freshwater discharge until it collapses (Figures 1a, 1a, 1e, 2a, and 2e). As the freshwater forcing is reduced, the circulation stays in a collapsed state only for a short period (less than 400 years in OBS and less than 200 years in LGM) before it starts to linearly strengthen. However, in the case of CBS, the AMOC exhibits a pronounced hysteresis behavior. It weakens with the enhancing of freshwater discharge, and the rate of weakening becomes accelerated as the freshwater forcing exceeds about 0.3 Sv. Then, the circulation collapses for a freshwater forcing of 0.42 Sv and continues to be collapsed for about 1400 years (Figure 2c) before it finally returns to a "conveyor belt" state.

[10] To explain these different AMOC hysteresis behaviors, we first resort to the AMOC stability indicator M_{ovS} and ΔM_{ov}. Here we make a brief review on the indicator ΔM_{ov}. In an equilibrium state, the overturning component of freshwater transport via a section is as follows:

$$M_{\mathrm{ov}} = (-1/S_0)\iint \langle v(x,z)\rangle(\langle s(x,z)\rangle - S_0)dxdz$$

where v is the normal velocity and s is the salinity. The angle bracket indicates the along-section mean. S_0 is a reference salinity, which is taken as the basin mean salinity in the Atlantic and appears to be time dependent in three hysteresis experiments (Figure S1, SI text 2). The indicator ΔM_{ov} is defined as $\Delta M_{\mathrm{ov}} = M_{\mathrm{ovS}} - M_{\mathrm{ovN}}$, where M_{ovS} and M_{ovN} are the AMOC freshwater transports at the southern (θ_S ~34°S) and northern (θ_N ~80°N; see Figures S2 and S3, SI text 3) boundaries, and the latter equals to the sum of the overturning liquid freshwater transports across the Canadian Arctic Archipelago (CAA; M_{ovCAA}), the Fram Strait (M_{ovFRA}), and the western shelf of the Barents Sea (M_{ovBAR}). Note here M_{ov} is not sensitive to the choice of S_0 (Figure S4, SI text 2). Physically, ΔM_{ov} represents a basin-scale salinity-advection feedback so that the AMOC is stable (with single equilibrium) when ΔM_{ov} is positive (freshwater convergence) but is unstable (with multiple equilibria) when ΔM_{ov} is negative (freshwater divergence). As shown in Figures 1 and 2, both indicators M_{ovS} and ΔM_{ov} cannot interpret the AMOC stability in the hysteresis loops. This is because, in response to the freshwater forcing, the sign of ΔM_{ov} (M_{ovS}) switches between positive and negative in all three experiments. Then, according to the theory, the AMOCs from all three experiments should have multiple equilibria and exhibit robust hysteresis behaviors when ΔM_{ov} is negative, which is obviously not true in the OBS and LGM cases.

[11] The reason for the failure of ΔM_{ov} and M_{ovS} is that neither of them becomes zero as the circulation collapses (Figures 1 and 2). The initial argument on the transport (convergence) indicator [*Rahmstorf*, 1996] is built on an idealized hypothesis that, when the AMOC collapses, the circulation is completely shut down and will no longer induce any freshwater transport (convergence) across the Atlantic basin, i.e., $M_{\mathrm{ovS}} = 0$ ($\Delta M_{\mathrm{ov}} = 0$). Following this hypothesis and taking ΔM_{ov} as an example, for an active AMOC inducing a positive/negative ΔM_{ov} (freshwater

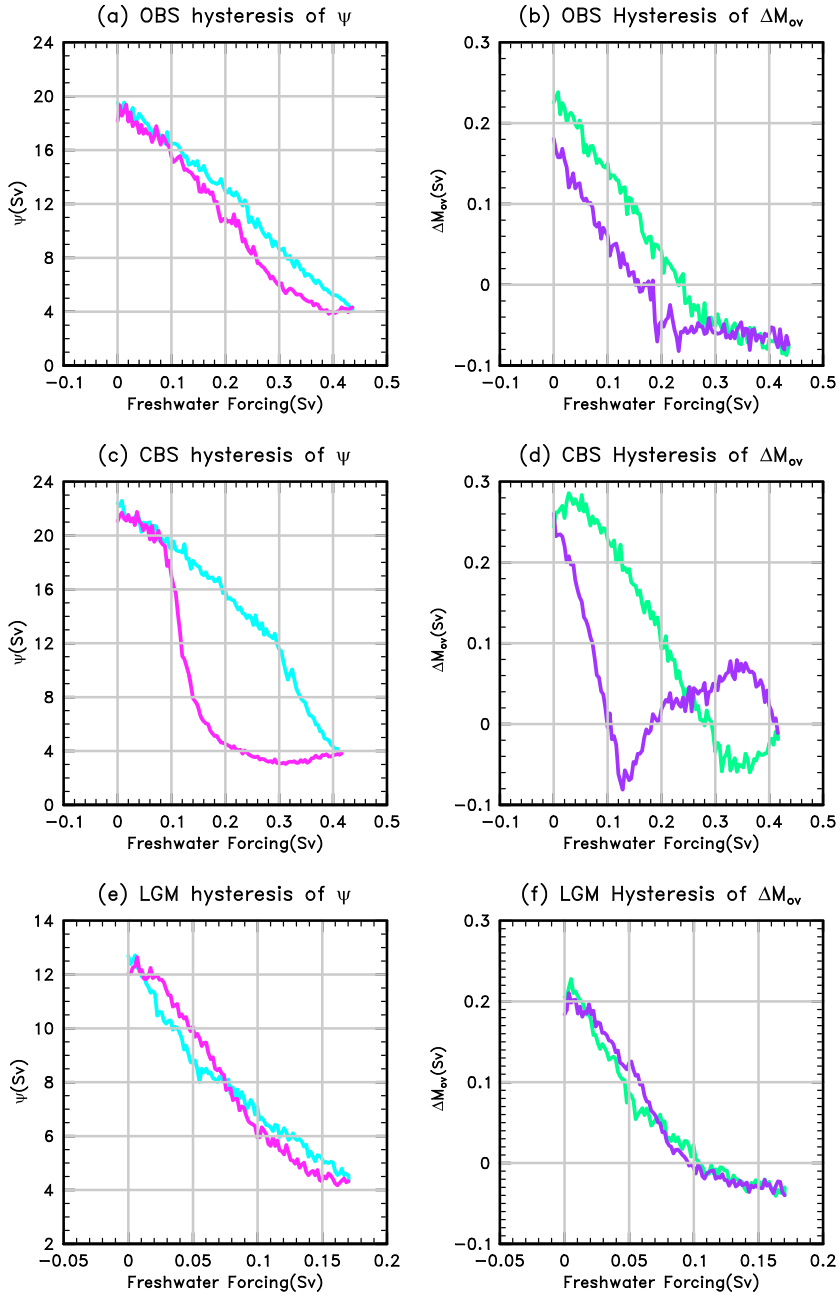

Figure 1. (left) Hysteresis diagrams of the AMOC strength ψ in the (a) OBS, (c) CBS, and (e) LGM simulations. The cyan (magenta) curves represent the phase of freshwater forcing increase (decrease) in these simulations. (right) Hysteresis diagrams of the net AMOC-induced freshwater transport ΔM_{ov} in the (b) OBS, (d) CBS, and (f) LGM simulations. The green (purple) curves represent the phase of freshwater forcing increase (decrease) in these simulations. ψ is defined as the maximum of the annual overturning stream function below 500 m depth in the North Atlantic and shown as a 20 year mean. ΔM_{ov} is calculated from monthly model output and also shown as a 20 year mean. Plots (a) and (c) are redrawn from *Hu et al*. [2012a].

convergence/divergence), the collapse of the circulation will cause a net salinity/freshwater accumulation in the Atlantic basin, which eventually results in the resumption/collapse of the AMOC [*de Vries and Weber*, 2005]. However, in most CGCMs (such as these two versions of CCSM3), the AMOC strength cannot reduce to zero due to the strong air-sea interaction in the North Atlantic. The collapsed AMOC usually appears as a clockwise North Atlantic Deep Water cell, with a minor strength of 3–4 Sv [cf. Figure 5 in *Hu et al*., 2012a], which may induce either a freshwater divergence ($\Delta M_{ov} < 0$, such as in OBS and LGM) or a freshwater convergence ($\Delta M_{ov} > 0$, such as in CBS). Thus, in this situation, the sign of ΔM_{ov} from an active AMOC cannot directly indicate the possible change of the net freshwater transport in basin when the circulation collapses and, in turn, the AMOC stability.

[12] Here we develop a generalized indicator of the AMOC stability $L = \partial \Delta \bar{M}_{ov} / \partial \bar{\psi}$ (SI text 4), and $\bar{\psi}$ and $\Delta \bar{M}_{ov}$ are the AMOC strength and the AMOC-induced freshwater transport convergence from an equilibrium state.

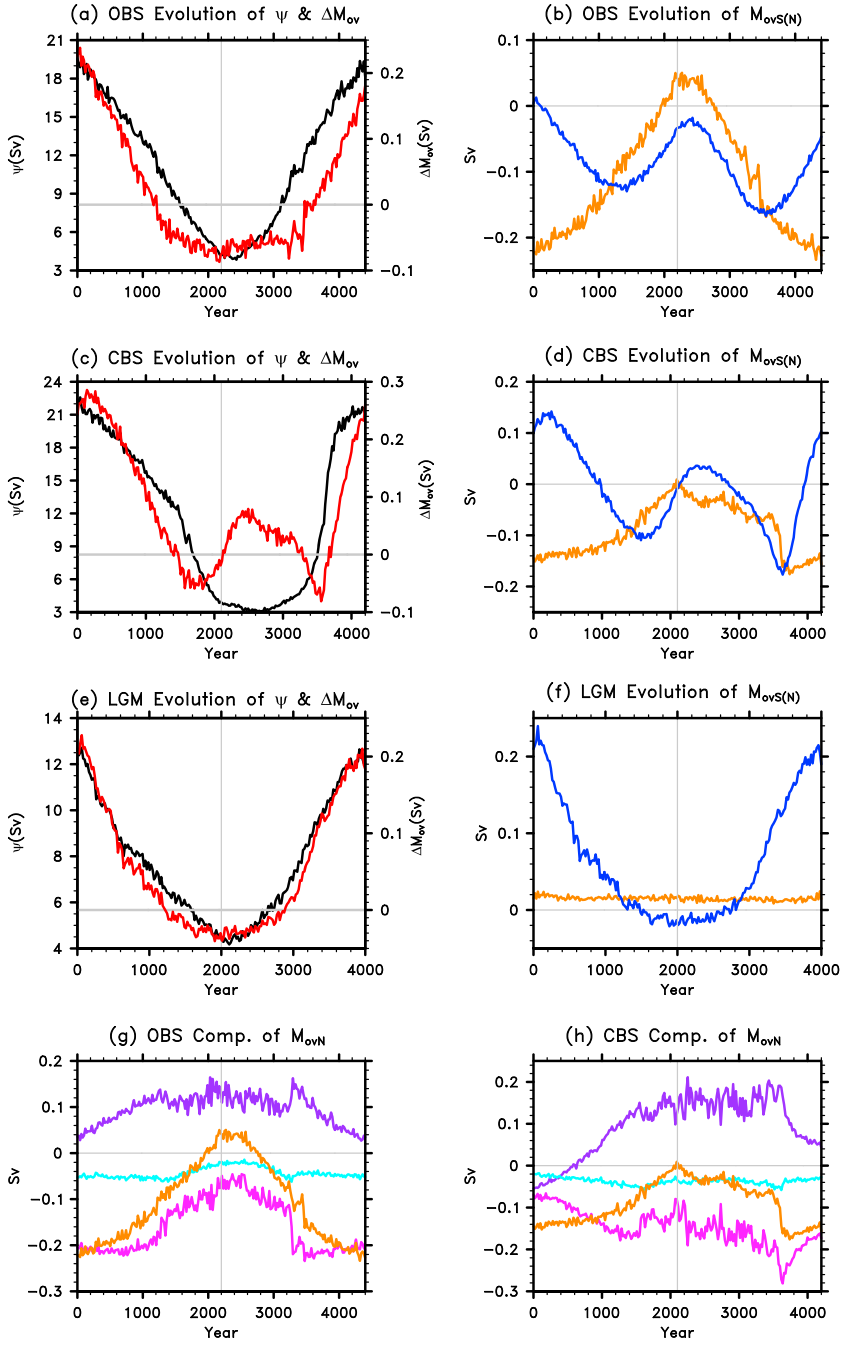

Figure 2. (left, top three plots) Evolution of the AMOC strength ψ (black) and the net AMOC-induced freshwater transport ΔM_{ov} (red) in the (a) OBS, (c) CBS, and (e) LGM simulations. (right, top three plots) Evolution of the AMOC-induced freshwater transports at the southern (M_{ovS}, blue) and northern (M_{ovN}, orange) boundaries in the (b) OBS, (d) CBS, and (f) LGM simulations. (bottom row) Evolution of M_{ovN} (orange) and the M_{ovN} components, i.e., the liquid overturning freshwater transports across the Fram Strait (M_{ovFRA}, magenta), the CAA (M_{ovCAA}, cyan), and the western shelf of the Barents Sea (M_{ovBAR}, purple) in the (f) OBS and (g) CBS simulations. In the LGM simulation, $M_{ovN} = M_{ovFRA}$ since the CAA and the Barents Sea are closed. In the figure, ψ and all the freshwater transports are shown as the 20 year means.

Unlike ΔM_{ov}, L is more generalized in showing how the Atlantic freshwater transport changes when the AMOC transits from one equilibrium to another. More importantly, in the definition of L, the AMOC-induced freshwater transport does not have to be zero for a collapsed AMOC. When L 0, it represents a negative feedback and indicates a stable AMOC. Starting from an equilibrium state, an initial weakening (strengthening) of the AMOC will induce an anomalous freshwater convergence (divergence) and salinify (freshen) the Atlantic basin, which then enhances (reduces) the deep convection and in turn prevents a further weakening (strengthening) of the AMOC. On the other hand, when $L < 0$, it represents a positive feedback. The initial weakening (strengthening) of the AMOC will be amplified by a basin-wide salt-advection feedback, suggesting that the circulation is in an unstable regime.

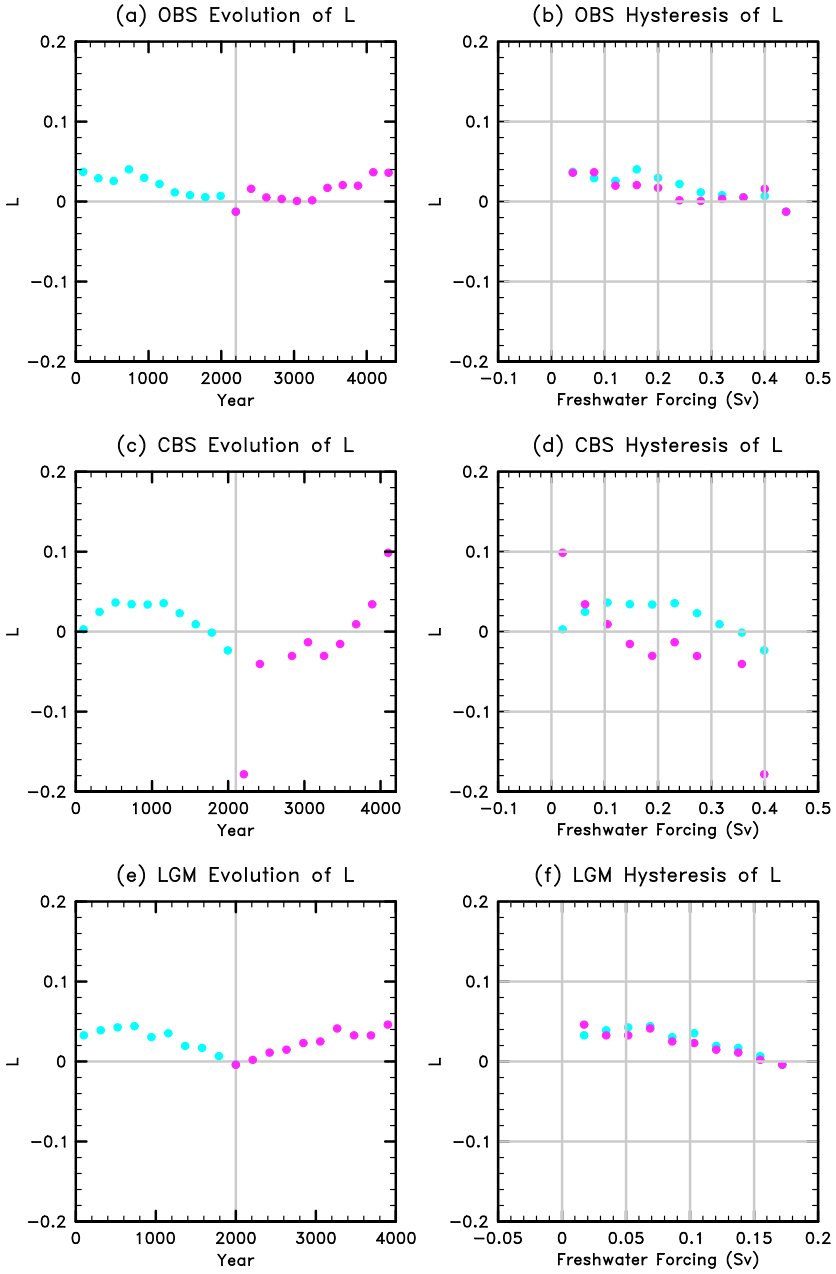

Figure 3. (left) Evolution of the generalized AMOC stability indicator $L = \partial\overline{\Delta M_{ov}}/\partial\bar{\psi}$ in the (a) OBS, (c) CBS, and (e) LGM simulations. (right) Hysteresis diagrams of L in the (b) OBS, (d) CBS, and (f) LGM simulations. In all plots, the cyan/magenta dots represent the phase of freshwater forcing increase (decrease) in simulations. $\bar{\psi}$ and $\overline{\Delta M_{ov}}$ are taken as the 200 year mean of ψ and ΔM_{ov} in the calculation of L.

[13] This generalized indicator L helps us to explicitly explain the stability of the evolving AMOCs among three experiments. In OBS and LGM, L is generally positive (Figures 3a, 3b, 3e, and 3f), which correctly indicates that the AMOCs in these two cases always reside in a stable regime and thus with single equilibrium. However, the case is different in CBS, where L becomes negative in year 1600–3600 as the freshwater forcing increases from 0.32 to 0.42 Sv and then drops to 0.12 Sv (Figures 3c and 3d). During this period, the AMOC has an unstable response to the hosing perturbation and exhibits multiple equilibria under the same freshwater forcing. Here it is worth mentioning that, in the calculation of L, $\bar{\psi}$ and $\Delta\bar{M}_{ov}$ are taken as the 200 year mean values to eliminate the AMOC interdecadal variability, and the sign of L is not sensitive to the averaging span of ψ and ΔM_{ov} as long as it is beyond the interdecadal time scale (Figure S4, SI text 5).

[14] Based on the indicator L, we found that differences in the AMOC stability among three experiments are derived from different responses of M_{ovS} and M_{ovN} to the freshwater hosing. In OBS and CBS, both M_{ovS} exhibit a similar saddle-like evolution pattern (Figures 2b and 2d) as a result of subtle changes in the salinity field at 34°S (Figures S6a and S6b, SI text 6). On the other hand, due to the Bering Strait (BS) effect under the present-day climate [*Hu and Meehl*, 2005; *Hu et al.*, 2007, 2008], M_{ovN} in OBS and

CBS exhibits different evolution patterns, which further results in different ΔM_{ov}, in turn, the AMOC stability in these two cases. In OBS, with the increasing freshwater discharge, the BS throughflow weakens or even reverses its direction [cf. Figure S2 in *Hu et al*., 2012a], which makes the Arctic freshwater export decrease significantly (mainly via the Fram Strait and the western Barents Sea, see Figure 2f) or even reverse the direction at the maximum hosing (Figure 2b). This diverging effect via M_{ovN} dominates the change of ΔM_{ov} when the AMOC approaches collapse (Figures 2a and 2b), and it enables the AMOC readily to ecover as long as the freshwater forcing starts to decrease. Alternatively, a closed BS eliminates the BS throughflow and then diminishes the diverging effect via M_{ovN}. Comparing with OBS, the Arctic freshwater export in CBS has a smaller reduction and never reverses its direction with enhanced freshwater forcing (Figure 2d). As a result, changes in M_{ovN} have a minor effect on the evolution of ΔM_{ov}, and the latter is largely determined by the evolution of M_{ovS}. In this case, when the AMOC approaches collapse, freshwater converges into the Atlantic basin and accumulates in the North Atlantic, which inhibits the deep convection, making the circulation stay in a stable collapsed state over 1000 years even after the freshwater hosing begins to decrease. In brief, under the present-day climate, a closed BS induces instability of the AMOC and leads to the hysteresis behavior of the circulation.

[15] However, the BS effect on the AMOC may depend on the background climate state. Although both CBS and LGM adopt a BS closure setting, unlike CBS, $M_{ovN} > 0$ in LGM since, during the glacial period, freshwater is imported into the Arctic from the North Atlantic to balance the sea ice export from the former to the latter [*Hu et al*., 2008]. In response to enhanced freshwater hosing, M_{ovN} keeps a small amplitude of about 0.02 Sv, with little change during the whole simulation. Meanwhile, the freshwater import at the southern boundary (M_{ovS}) monotonically decreases from ~0.23 to 0 Sv and switches into freshwater export at the maximum hosing, as a result of continuously freshening in the upper ocean over there (Figure S6c). Therefore, the much colder climate during the LGM may have partly mitigated the BS effect on the AMOC hysteresis, and the evolution pattern of ΔM_{ov} is almost entirely determined by M_{ovS}.

4. Conclusion

[16] In this study, a generalized indicator L is proposed to indicate the stability of the slow-evolving and quasi-steady AMOCs in three hysteresis experiments by CGCMs, which represents a feedback associated with the AMOC and its freshwater transport within the Atlantic basin. In the OBS and LGM simulations, L is generally positive, suggesting that the AMOCs in these two simulations stay in a stable regime and therefore have single equilibrium. However, L falls into negative in the CBS simulation, which indicates that the AMOC has an unstable response to the hosing perturbation, with characteristics of multiple equilibria. Based on the indicator L, further analysis shows that in the present-day climate, the BS plays an important role in regulating the AMOC stability. However, the BS effect is much reduced under the LGM climate.

[17] This generalized indicator L has great implications for the paleoclimate studies. By using the indicator L, we can diagnose the AMOC stability over a certain slowly evolving period in the past climate to understand the subsequent abrupt climate change due to instability of the circulation (such as the Heinrich event 1, Bolling-Allerod transitions).

[18] Meanwhile, it is worth noting that, in numerical models, L is a better indicator for the stability of the AMOC than M_{ovS} or ΔM_{ov}, since it acts as a true feedback term. However, in observations, values of M_{ovS} or ΔM_{ov} are more easily estimated than L, and in most cases, as we expect, L and M_{ovS} or ΔM_{ov} should behave similarly as long as the AMOC is at a quasi-equilibrium state.

[19] Finally, we should mention that we did not perform the freshwater compensation outside the hosing area in three simulations in order to follow the natural deglaciation process during the long-term glacial-interglacial cycles. However, the lack of compensation may induce several issues in the model scenarios. First, the BS feedback is likely to be influenced by the lack of hosing compensation in the Indo-Pacific. Also, the model could deviate from its equilibrium to some extent due to a failure of salt conservation over the global ocean (the deviation is small in this study). Besides, the freshwater compensation may not make a difference for the evolution of the AMOC; however, it may strongly affect the freshwater transport related to the AMOC, and the wellness of ΔM_{ov} and L as an indicator for the stability of the AMOC.

[20] **Acknowledgments.** This study is supported by the Priority Academic Program Development of Jiangsu Higher Education Institutions (PAPD). The authors thank Guangshan Chen for his support in the data processing. Also, this study was supported by the Office of Science (BER), U. S. DOE, Cooperative Agreement No. DE-FC02-97ER62402, as well as U. S. NSF and Chinese NSF: NSFC 41130105. NCAR is sponsored by the U.S. NSF. The resources used at NERSC are supported by the Office of Science of the U.S. DOE under Contract DE-AC02-05CH11231 as well as the NERSC project: m1382.

References

Bond, G. et al. (1997), A pervasive millennial-scale cycle in North Atlantic Holocene and glacial climates, *Science*, *278*, 1257–1266, doi:10.1126/science.278.5341.1257.

Broecker, W. S. et al. (1985), Does the ocean–atmosphere system have more than one stable mode of operation?, *Nature*, *315*, 21–26, doi:10.1038/315021a0.

Bryan, F. (1986), High-latitude salinity effects and interhemispheric thermohaline circulations, *Nature*, *323*, 301–304.

Collins, W. D. et al. (2006), The Community Climate System Model version 3 (CCSM3), *J. Clim.*, *19*, 2122–2143.

Dansgaard, W. et al. (1993), Evidence for general instability of past climate from a 250-kyr ice-core record, *Nature*, *364*, 218–220.

de Vries, P., and S. L. Weber (2005), The Atlantic freshwater budget as a diagnostic for the existence of a stable shut down of the meridional overturning circulation, *Geophys. Res. Lett.*, *32*, L09606, doi:10.1029/2004GL021450.

Dijkstra, H. A. (2007), Characterization of the multiple equilibria regime in a global ocean model, *Tellus*, *59A*, 695–705.

Ganachaud, A., and C. Wunsch (2000), Improved estimates of global ocean circulation, heat transport and mixing from hydrographic data, *Nature*, *408*, 453–456.

Hawkins, E., et al. (2011), Bistability of the Atlantic overturning circulation in a global climate model and links to ocean freshwater transport, *Geophys. Res. Lett.*, *38*, L10605, doi:10.1029/2011GL047208.

Hofmann, M., and S. Rahmstorf (2009), On the stability of the Atlantic meridional overturning circulation, *Proc. Natl. Acad. Sci. U. S. A.*, *106*, 20584–20589.

Hu, A., and G. A. Meehl (2005), Bering Strait throughflow and the thermohaline circulation, *Geophys. Res. Lett.*, *32*, L24610, doi:10.1029/2005GL024424.

Hu, A., et al. (2007), Role of the Bering Strait in the thermohaline circulation and abrupt climate change, *Geophys. Res. Lett.*, *34*, L05704, doi:10.1029/2006GL028906.

Hu, A. et al. (2008), Response of thermohaline circulation to freshwater forcing under present day and LGM conditions, *J. Clim.*, *21*, 2239–2258.

Hu, A., et al. (2012a), Role of the Bering Strait on the hysteresis of the ocean conveyor belt circulation and glacial climate stability, *Proc. Natl. Acad. Sci. USA*, www.pnas.org/cgi/doi/10.1073/pnas.1116014109.

Hu, A., et al. (2012b), The Pacific-Atlantic Seesaw and the Bering Strait, *Geophys. Res. Lett.*, *39*, L03702, doi:10.1029/2011GL050567.

Huisman, S. E. et al. (2010), An indicator of the multiple equilibria regime of the Atlantic meridional overturning circulation, *J. Phys. Oceanogr.*, *40*, 551–567.

Liu, W. (2012), Insights from deglacial changes in the Southern Ocean and Atlantic Meridional Overturning Circulation during the last deglaciation, PhD thesis, 150 pp., Univ. of Wisconsin-Madison, Wis.

Liu, W., and Z. Liu (2013), A diagnostic indicator of the stability of the Atlantic Meridional Overturning Circulation in CCSM3, *J. Clim.*, *26*, 1926–1938.

Liu, Z. et al. (2009), Transient simulation of last deglaciation with a new mechanism for Bølling-Allerød warming, *Science*, *325*, 310–314.

Manabe, S., and R. J. Stouffer (1988), Two stable equilibria of a coupled ocean-atmosphere model, *J. Clim.*, *1*, 841–866.

Marotzke, J. et al. (1988), Instability and multiple steady states in a meridional-plane model of the thermohaline circulation, *Tellus*, *40A*, 162–172.

McManus, J. F. et al. (2004), Collapse and rapid resumption of Atlantic meridional circulation linked to deglacial climate changes, *Nature*, *428*, 834–837.

Rahmstorf, S. (1995), Bifurcations of the Atlantic thermohaline circulation in response to changes in the hydrological cycle, *Nature*, *378*, 145–149.

Rahmstorf, S. (1996), On the freshwater forcing and transport of the Atlantic thermohaline circulation, *Clim. Dyn.*, *12*, 799–811.

Rahmstorf, S., et al. (2005), Thermohaline circulation hysteresis: A model intercomparison, *Geophys. Res. Lett.*, *32*, L23605, doi:10.1029/2005GL023655.

Rooth, C. (1982), Hydrology and ocean circulation, *Prog. Oceanogr.*, *11*, 131–149.

Severinghaus, J. P., and E. J. Brook (1999), Abrupt climate change at the end of the last glacial period inferred from trapped air in polar ice, *Science*, *286*, 930–934.

Stommel, H. (1961), Thermohaline convection with two stable regimes of flow, *Tellus*, *2*, 244–230.

Tziperman, E. et al. (1994), Instability of the thermohaline circulation with respect to mixed boundary conditions: Is it really a problem for realistic models?, *J. Phys. Oceanogr.*, *24*, 217–232.

Weaver, A. J., and E. S. Sarachik (1991), The role of mixed boundary conditions in numerical models of the ocean's climate, *J. Phys. Oceanogr.*, *21*, 1470–1493.

Yeager, S. G. et al. (2006), The low-resolution CCSM3, *J. Clim.*, *19*, 2545–2566.

Yin, J., and R. J. Stouffer (2007), Comparison of the stability of the Atlantic thermohaline circulation in two coupled atmosphere–ocean general circulation models, *J. Clim.*, *20*, 4293–4315.